DOKUZ EYLÜL UNIVERSITY

GRADUATE SCHOOL OF NATURAL AND APPLIED SCIENCES

INVESTIGATION OF DESIGN PARAMETERS EFFECTS OF AN ACTIVE SUCTION COOLING SYSTEM ON OUTER SURFACE TEMPERATURE OVEN GLASS AT A PYROLITIC OVEN

by

Berrin EKER

March, 2016

İZMİR

INVESTIGATION OF DESIGN PARAMETERS EFFECTS OF AN ACTIVE SUCTION COOLING SYSTEM ON OUTER SURFACE TEMPERATURE OVEN GLASS AT A PYROLITIC OVEN

A Thesis Submitted to the
Graduate School of Natural and Applied Sciences of Dokuz Eylül University
In Partial Fulfillment of the Requirements for the Degree of Master of Science
in Mechanical Engineering, Energy Program

by

Berrin EKER

March, 2016

İZMİR

M.Sc THESIS EXAMINATION RESULT FORM

We have read the thesis entitled **"INVESTIGATION OF DESIGN PARAMETERS EFFECTS OF AN ACTIVE SUCTION COOLING SYSTEM ON OUTER SURFACE TEMPERATURE OVEN GLASS AT A PYROLITIC OVEN"** completed by **BERRİN EKER** under supervision of **PROF. DR. DİLEK KUMLUTAŞ** and we certify that in our opinion it is fully adequate, in scope and in quality, as a thesis for the degree of Master of Science.

Prof. Dr. Dilek KUMLUTAŞ

Supervisor

Prof. Dr. İsmail Tosun

(Jury Member)

Prof. Dr. Aydoğan Özdamar

(Jury Member)

Prof.Dr. Ayşe OKUR
Director
Graduate School of Natural and Applied Sciences

ACKNOWLEDGEMENTS

First of all, I would like to thank my supervisor, Prof. Dr. Dilek KUMLUTAŞ, for her incomparable knowledge and moral support, valuable advises and guidance throughout this thesis study.

I also wish to express my gratitude to Project Assistant Özgün ÖZER for his motivation, support and sharing their valuable experiences with me.

Also, I would like to express special thanks to my friends for their motivation and help.

Finally, I would like thank to my family for their invaluable support, encouragement and patience throughout my entire life.

Berrin EKER

INVESTIGATION OF DESIGN PARAMETERS EFFECTS OF AN ACTIVE SUCTION COOLING SYSTEM ON OUTER SURFACE TEMPERATURE OVEN GLASS AT A PYROLYTIC OVEN

ABSTRACT

The aim of this study is to investigate effects of an active suction cooling (ASC) system on outer surface temperature of oven glass at a pyrolytic oven which are used commonly at households. Pyrolytic ovens include complicated components, such as the oven door and cross-flow fan (CFF), ASC unit and their complex interaction needs to be investigated in detail. In this study, oven door, CFF and ASC unit were modeled together as a three dimensional using computational fluid dynamics and heat transfer (CFDHT) method, fluid flow and temperature distribution of oven doors' outer surface was investigated. The numerical results were validated by comparing with the results obtained from experimental study. The simulation model was predicted this temperature distribution for the parameter' value, namely the rotational speed of CFF. The calculated computational results show that the CFF speed plays an important role in outer surface temperature of oven glass at a pyrolytic oven.

The success of this study is to develop an investigation method of heat transfer and fluid flow characteristics for pyrolytic ovens.

Keywords: Computational fluid dynamics and heat transfer (CFD), household ovens, pyrolytic, active suction cooling system

PİROLOTİK BİR FIRINDA AKTİF ÇEKİŞLİ SOĞUTMA SİSTEM TASARIMININ FIRIN DIŞ CAM SICAKLIĞINA ETKİSİNİN İNCELENMESİ

ÖZ

Bu çalışmanın amacı; evlerde yaygın olarak kullanılan pirolitik fırınlardaki aktif çekiş sisteminin kapı dış cam yüzey sıcaklığına olan etkisinin incelenmesidir. Pirolitik fırınlar fırın kapısı, çapraz akışlı fan, aktif çekişli soğuma ünitesi gibi karmaşık elemanlar içermektedir, bu elemanlar ve etkileşimleri detaylı olarak incelenmelidir. Bu çalışmada fırın kapısı, çapraz akışlı fan ve aktif çekişli soğutma sistemi üç boyutlu olarak birlikte modellenmiş olup hesaplamalı akışkanlar dinamiği ve ısı transferi (HADIT) kullanılarak modellenmiş, hava akış yapısı ve fırın kapısı dış camı üzerindeki sıcaklık dağılımı incelenmiştir. Sayısal sonuçlar deneysel çalışmalardan elde edilen sonuçlarla karşılaştırılarak doğrulanmıştır. Parametrik çalışma olarak çapraz akışlı fan devrinin kapı dış yüzey sıcaklığına olan etkisi incelenmiştir. Bu çalışma sonucunda fan devrinin kapı dış sıcaklığı üzerinde önemli bir rol oynadığı görülmüştür.

Bu çalışmanın başarısı ev tipi pirolitik fırınların ısı ve akış transferi karakteristiklerini inceleyecek bir yöntem geliştirilmesidir.

Anahtar kelimeler: Hesaplamalı akışkanlar dinamiği ve ısı transferi (HADIT), ev tipi fırınlar, pirolitik, aktif çekişli soğutma sistemi

CONTENTS

Page

LIST OF FIGURES

Page

LIST OF TABLES

Page

CHAPTER ONE
INTRODUCTION

1.1 Literature Survey

In the design of domestic ovens, one of the most important parameters is outer glass temperature. Especially in pyrolytic type domestic ovens, due to high temperatures outer glass temperature is a big factor in design process. By computational fluid dynamics and heat transfer (CFDHT) method, time and cost both can be saved. In this study, using the numerical methods, a household pyrolytic oven door driven by an active-suction-cooling system is analysed. After the results of the numerical study are verified experimentally and critical parameters of door design are determined.

Pyrolytic ovens have a self-cleaning function which happens by heating inside of the oven that increase over 500 ^{0}C. When the temperatures' inside of the oven reach this values, any food residue and grime stuck to the walls is simply burned off. This feature provides great convenience for users but, because of high-temperature, the thermal design is very important.

One of the most important points in terms of design is safety. For that reason, the outer surfaces' temperature of the oven should be reduced the level that will not harm the environment and other living things. The insulation is very important parameter, not only this reason but also energy efficiency.

For reducing temperature of outer surfaces' oven door is designed active suction cooling (ASC) system as well as insulation. This system provides air through the door between panes, thereby reducing the door's external surface temperature. The providing cooling is via convection. In this instance, velocity of suction air which and design of oven door are very important. If the cooling is not suitable, the temperatures' inside of the oven could reduce. This case can damage to cooking quality and energy efficiency.

Chhanwal, Anishaparvin, Indrani, Raghavarao, & Anandharamakrishnan (2010) studied on an electric heating baking oven for bread baking process. They simulated three different radiation models; discrete transfer radiation model (DTRM), surface to surface (S2S) and discrete ordinate (DO). All models predicted almost similar results, DO radiation model was selected for bread baking simulation and validated with the experimental measurement of bread temperature. Their analysis is transient analysis.

Rek, Rudolf, & Zun (2012) modeled new generation oven. Oven was multifunctional. They modeled radiation, conduction; natural and forced convection mechanisms of heat transfer. They used discrete ordinate model used for radiation and described the density of air by incompressible ideal gas equation in a natural convection model. They worked up creating the best possible baking conditions for 5 different heating systems. They investigated many parameters which have influence on the conditions inside the oven, such as: the shape and power of heaters, fan rotor rotational speed, thickness and quality of insulation, the design of oven doors, etc. After their optimizations, they changed oven cavity geometry.

Abraham, & Sparrow (2004) developed algebraic method for the prediction of the time wise temperature variation of a thermal load situated in an electrically heated oven. The method included both natural convection within the oven cavity and radiation between the thermal load and the oven walls. The model provides a complete description of heat transfer external to the thermal load. It can be used to provide boundary conditions for an analysis of thermal loads of various heat-conducting characteristics. This method is able to accommodate loads of various shapes, sizes, materials, and radiation surface finishes, as well as oven heating conditions characterized by a wide range of oven set-point temperatures. The model was able to accommodate loads of various shapes, sizes, materials, and radiation surface finishes. They performed experiments to validate the predictive method. Measurements were transient response of the thermal load. And they collected temperature data from the oven walls. Among the walls, the temperatures on the

oven door were the lowest, whereas the highest temperatures were encountered on the oven floor and on the top wall.

Mistry, Ganapathi-subbu, Dey, Bishnoi, & Castillo (2006) studied transient natural convection heat transfer in ovens. The CFD modeling of electric oven involves three dimensional, unsteady, natural convective flow-thermal field coupled with radiative heat transfer. The front doors have a double glazed window, which helps the operator to monitor the cooking without opening the door. They had a Tin oxide coated inner glass walls to ensure low transmissivity for reduced radiation losses. For radiation models, they studied on the discrete ordinate (DO) and surface-to-surface (S2S) radiation models. The DO model takes into account media participation in addition to the surface-to-surface radiation effects. But surface-to-surface radiation model considers only surface-to-surface radiation effects. But they found the difference of temperature prediction at the center of the oven and oven walls by the DO and S2S models for a simplified but similar geometry were of the order of 0.2%. Although the comparison of the thermal field was similar, the computational time for S2S model was almost half of the DO model for an identical grid.

In the study of Mistry, Ganapathisubbu, Dey, Bishnoi, & Castillo (2011), they have developed a CFD based methodology to evaluate performance of a domestic gas oven. This involves modeling three-dimensional, unsteady, forced convective flow field coupled with radioactive participating media. The gas oven of this study is shown in Figure 1.1.

For capturing transient heat transfer coupled with mixed convection flow field are evaluated considering the trade-off between computational time and accuracy of predictions. The results of this study showed 6% discrepancy with experimental data.

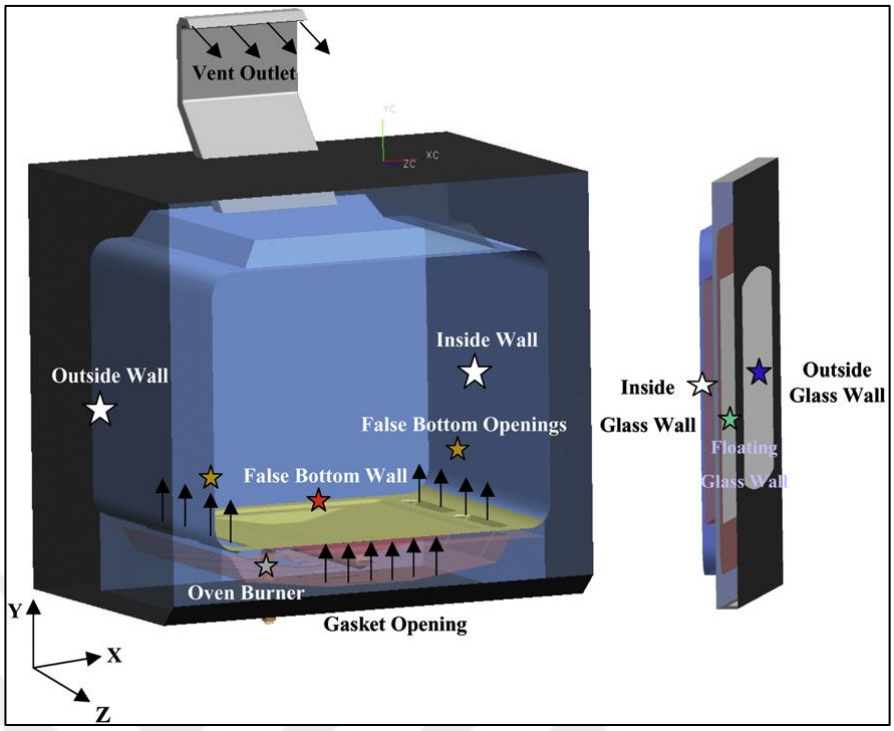

Figure 1.1 The gas oven (Mistry, Ganapathisubbu, Dey, Bishnoi, & Castillo, 2011)

Fahey, Wakes, & Shaw (2008) studied cooling on circuit of the door of a pyrolytic oven. They used experimental and numerical methods for examining the flow behavior of the oven. The CFD results were validated with experimental hot-wire velocity measurements. They investigated cooling system of the oven door.

In the study of Verboven, Scheerlinck, Baerdemaeker, & Nicolai (2000), they have investigated the forced convection in an oven using CFD methods. They have compared the numerical results of their study with experimental results of the oven. The heaters and fan of the oven of their study has not been modelled to reduce the computing cost for the analysis. The oven of this study has different airflow inlets than the typical ovens which are located at the sides of the oven. The heat transfer coefficients in this study have been computed more accurately by using turbulent boundary layer approach around the walls of the oven.

In the study of Smolka, Nowak, & Rybarz (2009), they have investigated the forced convection inside a drying oven by using experimentally validated 3-D CFD analysis. The oven of this study used at a constant, spatially uniform temperature. To

improving temperature uniformity within the oven cavity, they have changed the parameters such as the rotational speed of the device fan, the effectiveness of the distribution gaps and the rate of heat generated in the electrical heaters. They have also changed the configurations such as the locations of the heaters, the fan and the fan baffle. By completing these processes, they have improved the temperature uniformity and validated the results with the experimental test of the modified prototype.

As mentioned in the literature, the CFDHT method is very successful for revealing and understanding complex flow characteristics. The 3D modelling of a device is essential for determining the air-side flow and heat transfer together. Therefore, in this study, an oven door, cross flow fan (CFF) and ASC unit model was introduced and heat transfer and fluid flow analysis was made to determine the temperature distribution of oven doors' outer surface and fluid flow of oven door and ASC system. For numerical study, 3D models of the oven door, CFF and the ASC system were prepared and CFDHT analyses were made. Conduction, convection and radiation heat transfer mechanisms are modeled. The numerical results were validated by comparing with the results obtained from experimental study. Oven door and ASC system are modelled together as 3D for the first time in this study. Following, oven door and ASC system were modeled together and temperature distribution was investigated. In order to reduce temperature on the outers' surface of oven door, the influence of fan speed parameter has been investigated numerically.

CHAPTER TWO
OVENS

2.1 Oven

An oven is a thermally insulated chamber used for the heating, baking or drying of a substance and most commonly used for cooking. There are many variations of this basic concept, but all types of ovens control the temperature of the oven cavity. Ovens often use a variety of methods to cook food. They can either heat the food that is being cooked from below (often seen in baking and roasting) or from the top (providing broiling ability). In order to provide faster, more even cooking, convection ovens use a small fan to blow hot air around the cooking chamber. There are several types of available kitchen ovens that vary in appearance and function.

2.1.1 Electric Ovens

Electric ovens effectively distribute heat while being powered by electricity, although this can often result in a higher heating cost for the consumer. Many prefer this type of oven because they tend to use dry heat, which helps prevent the build up of rust. Electric ovens also feature a thermostat that controls the oven's temperature electronically, and many have top, bottom, or rear grill elements. Electric ovens can take longer to heat, but they are relatively inexpensive in cost compared to other types of ovens.

In a conventional electric oven, the thermostat controls the heat in the middle of the oven so it is always slightly hotter at this position. Conventional ovens take a while to reach cooking temperature so they need to be pre-heated. Fan-assisted ovens differ from standard conventional electric ovens, only in that a fan distributes the heat around the cooking compartment. Fan ovens circulate the heat around the oven creating a more even temperature, this ensures that food is cooked evenly and cooking times are reduced from the conventional (non-fan) type.

2.1.2 Gas Ovens

For individuals who spend a lot of time in the kitchen, gas ovens are more economical in the long run, even though they are usually initially more expensive to purchase. These ovens tend to heat and cool down more quickly than other types of ovens do, allowing greater convenience for buyers who may need to bake in a hurry. Gas ovens are known to provide great control over the exact temperature of the oven, giving them the ability to heat evenly. Unlike electric ovens that utilize dry heat, gas ovens allow for additional moisture which may prevent baked goods from becoming hard and brittle before the inside of the food is fully cooked. Some gas ovens are controlled electronically by a thermostat, while others must be attached to a natural gas outlet.

2.1.3 Built-In Ovens

A built - in oven, also known as a wall oven, is a cooking appliance that is built directly into the wall of a kitchen. This style of oven differs from traditional oven units that are paired directly with a cooking range on top of the oven. Although a built-in oven does not feature a cooktop, this feature is often installed directly into the kitchen countertop at various heights. Built-in ovens may feature either an electric or a gas heating element.

2.1.4 Double Ovens

Double ovens feature two ovens stacked on top of or alongside one another, which allows them to cook at separate temperatures. This style of oven is beneficial for cooks who prepare large meals and need the versatility that two ovens offer. While one oven may be set at a low temperature suitable for cooking meat slowly, the other can be used at a higher temperature to quickly cook another dish.

2.1.5 Microwave Oven

A microwave is a kitchen appliance that cooks or heats food by dielectric heating. This is accomplished by using microwave radiation to heat water and other polarized molecules within the food. This excitation is fairly uniform, leading to food being adequately heated throughout - except in thick objects. A microwave oven has in it a magnetron, which is a radio transmitter. Basically, microwave energy in the magnetron causes the water molecules in the food to move. That motion causes the water molecules to move more rapidly, which heats the food. Microwave energy can only penetrate about an inch into the food, and after that, heating is caused by conduction, i.e. the heated area heats adjacent areas, etc. It does not "cook food from the inside out", but works by exciting the water molecules.

2.2 Self-cleaning Oven

A self-cleaning oven is an oven which uses high temperature approximately 500 degrees Celsius to burn off leftovers from baking, without the use of any chemical agents. The oven door locks while the pyrolytic cleaning cycle (which lasts for around 1.5-2 hours) is in progress, for safety reasons. Once the cleaning cycle has completed, the ash can be safely wiped away using only a damp cloth. The process of using heat and pressure to convert organic matter into ash is known as 'pyrolysis' - which is where pyrolytic ovens get their name. Self-cleaning ovens usually have more insulation than standard ovens to reduce the possibility of fire. The insulation also reduces the amount of energy needed for normal cooking.

The inside of the oven is heated and reaches 500° C, at which temperature any grease stuck to the walls is simply burned off. However, the quadruple glazing ensures that the outer door will become no hotter than 55ºC. The Pyrolytic cycle is carried out in total safety as a special safety device locks the door for the duration of the process.

CHAPTER THREE
COMPUTATIONAL FLUID DYNAMICS AND HEAT TRANSFER

3.1 History of Computational Fluid Dynamics and Heat Transfer

The history of Computational Fluid Dynamics, or CFD for short started in the early 1970's. Around that time, it became an acronym for a combination of physics, numerical mathematics, and, to some extent, computer sciences employed to simulate fluid flows. The beginning of CFD was triggered by the availability of increasingly more powerful mainframes and the advances in CFD are still tightly coupled to the evolution of computer technology. Among the first applications of the CFD methods was the simulation of transonic flows based on .the solution of the non-linear potential equation. With the beginning of the 1980's, the solution of first two-dimensional (2-D) and later also three-dimensional (3-D) Euler equations became feasible. Thanks to the rapidly increasing speed of supercomputers and due to the development of a variety of numerical acceleration techniques like multigrid, it was possible to compute inviscid flows past complete aircraft configurations or inside of turbomachines. With the mid 1980's, the focus started to shift to the significantly more demanding simulation of viscous flows governed by the Navier-Stokes equations. Together with this, a variety of turbulence models evolved with different degree of numerical complexity and accuracy. The leading edge in turbulence modelling is represented by the Direct Numerical Simulation (DNS) and the Large Eddy Simulation (LES). However, both approaches are still far away from being usable in engineering applications (Blazek, 2001).

Nowadays, CFD methodologies are routinely employed in the fields of aircraft, turbomachinery, car, and ship design. Furthermore, CFD is also applied in meteorology, oceanography, astrophysics, in oil recovery, and also in architecture. Many numerical techniques developed for CFD are used in the solution of Maxwell equations as well. Hence, CFD is becoming an increasingly important design tool in engineering and also a substantial research tool in certain physical sciences. Due to

the advances in numerical solution methods and computer technology, geometrically complex cases, like those which are often encountered in turbomachinery, can be treated. Also, large scale simulations of viscous flows can be accomplished within only a few hours on today's supercomputers, even for grids consisting of dozens of millions of grid cells. However, it would be completely wrong to think that CFD represents a mature technology now, like for example structural finite element methods. No, there are still many open questions like turbulence and combustion modelling, heat transfer, efficient solution techniques for viscous flows, robust but accurate discretisation methods, etc. Also the connection of CFD with other disciplines (like structural mechanics or heat conduction) requires further research. Quite new opportunities also arise in the design optimisation by using CFD.

3.2 Mathematical Description of Flow

The derivation of the principal equations of fluid dynamics is based on the fact that the dynamical behaviour of a fluid is determined by the following conservation laws, namely:

1. The conservation of mass,
2. The conservation of momentum, and
3. The conservation of energy.

3.2.1 Finite Volume Control

An arbitrary finite region of the flow, bounded by the closed surface $\partial\Omega$ and fixed in space, defines the control volume Ω. We also introduce a surface element as dS and its associated, outward pointing unit normal vector as $\vec{n}$.

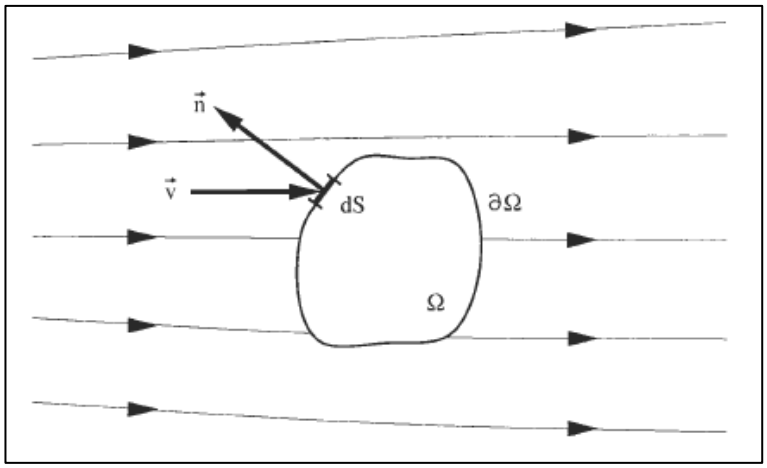

Figure 3.1 Definition of a control volume (fixed in space) (Blazek, 2001)

The conservation law applied to an exemplary scalar quantity per unit volume *U* now says that its variation in time within Ω, i.e.,

$$\frac{\partial}{\partial t}\int_{\Omega} U \, d\Omega \tag{3.1}$$

is equal to the sum of the contributions due to the convective flux – amount of the quantity U entering the control volume through the boundary with the velocity $\vec{v}$ – hence U$\vec{v}$

$$-\oint_{\partial\Omega} U(\vec{v}.\vec{n})dS \tag{3.2}$$

due to the diffusive flux - expressed by the generalised Fick's gradient law

$$\oint_{\partial\Omega} \kappa\rho[\nabla(U/\rho)\,.\vec{n}]dS \tag{3.3}$$

where **κ** is the thermal diffusivity coefficient, and due to the volume as well as surface sources, Q_V, $\overrightarrow{Qs}$, i.e.,

$$\int_{\Omega} Q_V d\Omega + \oint_{\partial\Omega}(\overrightarrow{Qs}.\vec{n})dS \tag{3.4}$$

respectively. After summing the above contributions, we obtain the following general form of the conservation law for the scalar quantity *U*

$$\frac{\partial}{\partial t}\int_{\Omega} U\, d\Omega + \frac{\partial}{\partial t}\int_{\Omega} U\, d\Omega = \int_{\Omega} Q_V d\Omega + \oint_{\partial\Omega}(\overrightarrow{Qs}.\vec{n})dS \qquad (3.5)$$

where U^{*} denotes the quantity U per unit mass, i.e., U/ρ.

It is important to note that if the conserved quantity would be a vector instead of a scalar, the above Equation (3.5) would formally still be valid. But in difference, the convective and the diffusive flux would become tensors instead of vectors - $\overline{\overline{F_C}}$ the convective flux tensor and $\overline{\overline{F_D}}$ the diffusive flux tensor. The volume sources would be a vector, $\overrightarrow{Q_V}$, and the surface sources would change into a tensor $\overline{\overline{Q_S}}$. We can therefore write the conservation law for a general vector quantity $\vec{U}$ as

$$\frac{\partial}{\partial t}\int_{\Omega} \vec{U}\, d\Omega + \oint_{\partial\Omega}[(\overline{\overline{F_C}} - \overline{\overline{F_D}}).\vec{n}]dS = \int_{\Omega} \overrightarrow{Q_V} d\Omega + \oint_{\partial\Omega}(\overline{\overline{Q_S}}.\vec{n})dS \qquad (3.6)$$

The integral formulation of the conservation law, as given by the Equations (3.5) or (3.6), has two very important and desirable properties:

1. if there are no volume sources present, the variation of *U* depends solely on the flux across the boundary ∂Ω and not on any flux inside the control volume Ω;
2. this particular form remain valid in the presence of discontinuities in the flow field like shocks or contact discontinuities.

Because of its generality and its desirable properties, it is not surprising that the majority of CFD codes is based today on the integral form of the governing equations.

3.3 Conversation Laws

3.3.1 The Continuity Equation

In order to derive the continuity equation, the model of a finite control volume fixed in space is utilized as sketched in Fig. 3.1. At a point on the control surface, the flow velocity is $\vec{v}$, the unit normal vector is $\vec{n}$ and *dS* denotes an elemental surface area. The conserved quantity in this case is the density ρ. For the time rate of change of the total mass inside the finite volume Ω, there is

$$\frac{\partial}{\partial t}\int_{\Omega}\rho\, d\Omega \tag{3.7}$$

The mass flow of a fluid through some surface fixed in space equals to the product of (density) x (surface area) x (velocity component perpendicular to the surface). Therefore, the contribution from the convective flux across each surface element *dS* becomes

$$\rho(\vec{v}.\vec{n})\mathrm{dS} \tag{3.8}$$

Since by convection $\vec{n}$ always points out of the control volume, it can be mentioned of inflow if the product $(\vec{v}.\vec{n})$ is negative, and of *outflow* if it is positive and hence the mass flow leaves the control volume. As stated above, there are no volume or surface sources present. Thus, by taking into account the general formulation of Eq. (3.5), it can be written

$$\frac{\partial}{\partial t}\int_{\Omega}\rho\, d\Omega + \oint_{\partial\Omega}\rho(\vec{v}.\vec{n})\mathrm{dS} = 0 \tag{3.9}$$

This represents the integral form of the continuity equation - the conservation law of mass.

3.3.2 The Momentum Equation

The momentum equation can be derived by recalling the particular form of Newton's second law which states that the variation of momentum is caused by the net force acting on a mass element. For the momentum of an infinitesimally small portion of the control volume Ω (see Fig. 3.1) we have

$$\rho\vec{v}\, d\Omega \tag{3.10}$$

The variation in time of momentum within the control volume equals

$$\frac{\partial}{\partial t}\int_{\Omega} \rho\vec{v}\, d\Omega \tag{3.11}$$

Hence, the conserved quantity is here the product of density times the velocity, i.e.,

$$\rho\vec{v} = [\ \rho u, \rho v, \rho w\ ]^{T} \tag{3.12}$$

The convective flux tensor, which describes the transfer of momentum across the boundary of the control volume, consists in the Cartesian coordinate system of the following three components

x-component : $\rho u\, \vec{v}$

y-component : $\rho v\, \vec{v}$

z-component : $\rho w\, \vec{v}$

The contribution of the convective flux tensor to the conservation of momentum is then given by

$$\oint_{\partial\Omega} \rho\vec{v}.(\vec{v}.\vec{n})\mathrm{dS} \tag{3.13}$$

The diffusive flux is zero, since there is no diffusion of momentum possible for a fluid at rest. Two kinds of forces acting on the control volume can be identified like:

1. External volume or body forces, which act directly on the mass of the volume. These are for example gravitational, buoyancy, Coriolis or centrifugal forces. In some cases, there can be electromagnetic forces present as well.

2. Surface forces, which act directly on the surface of the control volume. They result from only two sources:

(a) The pressure distribution, imposed by the outside fluid surrounding

(b) The shear and normal stresses, resulting from the friction between the fluid and the surface of the volume.

From the above, it can be seen that the body force per unit volume, denoted as $\rho\overrightarrow{f_e}$, corresponds to the volume sources in Eq. (3.5). Thus, the contribution of the body (external) force to the momentum conservation is

$$\int_\Omega \rho\overrightarrow{f_e}\, d\Omega \tag{3.14}$$

The surface sources consist then of two parts - an isotropic pressure component and a viscous stress tensor $\bar{\bar{\tau}}$, i.e.,

$$\bar{\bar{Q}}s = -p\bar{\bar{I}} + \bar{\bar{\tau}} \tag{3.15}$$

with $\bar{\bar{I}}$ being the unit tensor. The effect of the surface sources on the control volume is sketched in Figure 3.2.

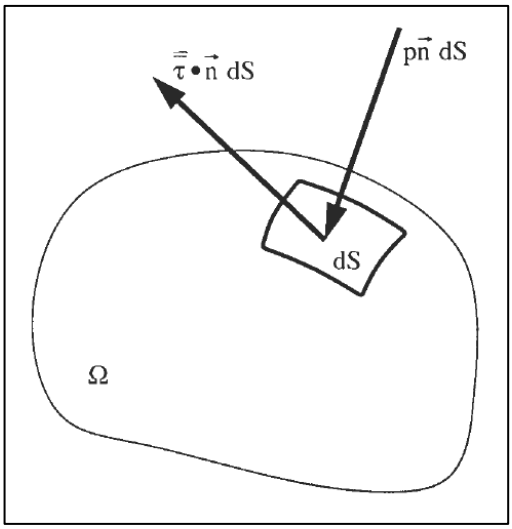

Figure 3.2 Surface forces acting on a surface element of the control volume (Blazek, 2001)

If all the above contributions according to the general conservation law is summed up (Eq. (3.6)), it is finally obtain the expression

$$\frac{\partial}{\partial t}\int_{\Omega}\rho\vec{v}\,d\Omega + \oint_{\partial\Omega}\rho\overrightarrow{v}.(\vec{v}.\vec{n})\mathrm{dS} = \int_{\Omega}\rho\overrightarrow{f_e}\,d\Omega - \oint_{\partial\Omega}p\vec{n}\,\mathrm{dS} + \oint_{\partial\Omega}(\bar{\bar{\tau}}.\vec{n})\,\mathrm{dS} \qquad (3.16)$$

For the momentum conservation inside an arbitrary control volume Ω which is fixed in space.

3.3.3 The Energy Equation

The underlying principle that it will be applied in the derivation of the energy equation is the first law of thermodynamics. Applied to the control volume displayed in Fig. 4.1, it states that any changes in time of the total energy inside the volume are caused by the rate of work of forces acting on the volume and by the net heat flux into it. The total energy per unit mass *E* of a fluid is obtained by adding its internal energy per unit mass, *e,* to its kinetic energy per unit mass, $|\vec{v}|^2$ / 2. Thus, it can be written for the total energy

$$E = e + \frac{|\vec{v}|^2}{2} + \frac{u^2+v^2+w^2}{2} \qquad (3.17)$$

The conserved quantity is in this case the total energy per unit volume, i.e., ρE. Its variation in time within the volume Ω can be expressed as

$$\frac{\partial}{\partial t}\int_{\Omega} \rho E \; d\Omega \tag{3.18}$$

Following the discussion in course of the derivation of the general conservation law (Eq. (3.5)), it can be readily specified the contribution of the convective flux as

$$\oint_{\partial\Omega} \rho E \; (\vec{v}.\vec{n}) \; \mathrm{dS} \tag{3.19}$$

In contrast to the continuity and the momentum equation, there is now a diffusive flux. It is proportional to the gradient of the conserved quantity per unit mass (Fick's law). Since the diffusive flux $\overrightarrow{F_D}$ is defined for fluid at rest, only the internal energy becomes effective and it is obtained

$$\overrightarrow{F_D} = -\gamma \; \rho \; \kappa \; \nabla \; e \tag{3.20}$$

In the above, $\gamma = \frac{c_p}{c_v}$ is the ratio of specific heat coefficients, and κ denotes the thermal diffusivity coefficient. The diffusion flux represents one part of the heat flux into the control volume, namely the diffusion of heat due to molecular thermal conduction - heat transfer due to temperature gradients. Therefore, Equation (3.20) is in general written in the form of Fourier's law of heat conduction, i.e.,

$$\overrightarrow{F_D} = -k \; \nabla \; T \tag{3.21}$$

with k standing for the thermal conductivity coefficient and T for the absolute static temperature.

The other part of the net heat flux into the finite control volume consists of volumetric heating due to absorption or emission of radiation, or due to chemical reactions. We will denote the heat sources - the time rate of heat transfer per unit

mass - as $\dot{q}_h$. Together with the rate of work done by the body forces $\overrightarrow{f_e}$, which we have introduced for the momentum equation, it completes the volume sources

$$Q_V = \rho\overrightarrow{f_e}.\vec{v} + \dot{q}_h \tag{3.22}$$

The last contributions to the conservation of energy, which we have yet to determine, are the surface sources Q_S. They correspond to the time rate of work done by the pressure as well as the shear and normal stresses on the fluid element

$$\overrightarrow{Q_S} = -p\vec{v} + \bar{\bar{\tau}}.\vec{v} \tag{3.23}$$

Sorting now all the above contributions and terms, we obtain for the energy conservation equation the expression

$$\frac{\partial}{\partial t}\int_\Omega \rho E \, d\Omega + \oint_{\partial\Omega} \rho E \, (\vec{v}.\vec{n}) \, dS = \oint_{\partial\Omega} k \, (\nabla T.\vec{n}) \, dS + \int_\Omega (\rho\overrightarrow{f_e}.\vec{v} + \dot{q}_h) \, d\Omega$$
$$- \oint_{\partial\Omega} p(\vec{v}.\vec{n}) \, dS + \oint_{\partial\Omega} (\bar{\bar{\tau}}.\vec{v}).\vec{n} \, dS \tag{3.24}$$

Usually, the energy equation (3.24) is written in a slightly different form. For that purpose, it will be utilised the following general relation between the total enthalpy, the total energy and the pressure

$$H = h + \frac{|\vec{v}|^2}{2} = E + \frac{p}{\rho} \tag{3.25}$$

When it is gathered the convective ($\rho E \vec{v}$) and the pressure term ($p\vec{v}$) in the energy conservation law (3.24) and apply the formula (3.25), it can be finally written the energy equation in the form

$$\frac{\partial}{\partial t}\int_\Omega \rho E \, d\Omega + \oint_{\partial\Omega} \rho H \, (\vec{v}.\vec{n}) \, dS = \oint_{\partial\Omega} k \, (\nabla T.\vec{n}) \, dS + \int_\Omega (\rho\overrightarrow{f_e}.\vec{v} + \dot{q}_h) \, d\Omega$$
$$+ \oint_{\partial\Omega} (\bar{\bar{\tau}}.\vec{v}).\vec{n} \, dS \tag{3.26}$$

Herewith, we have derived integral formulations of the three conservation laws: the conservation of mass (3.9), of momentum (3.16), and of energy (3.26).

CHAPTER FOUR
NUMERICAL STUDY

4.1 Introduction of Numerical Study

The domestic oven used in this study has been investigated with a two stage process. These stages are as follows:

Steady state thermal analysis of the ovens' door,

Steady state thermal analysis of the ovens' door and active suction system

The Computer Aided Design (CAD) model of the oven has been taken from a white goods company for the numerical study. The model is built-in oven which has pyrolytic function. The oven has ASC system for decreasing temperature of outer surfaces' oven door. The computer aided design (CAD) model of pyrolytic oven assembly is shown in Figure 4.1a. Details of ASC system and oven door are shown in Figure 4.1b and Figure 4.1c.

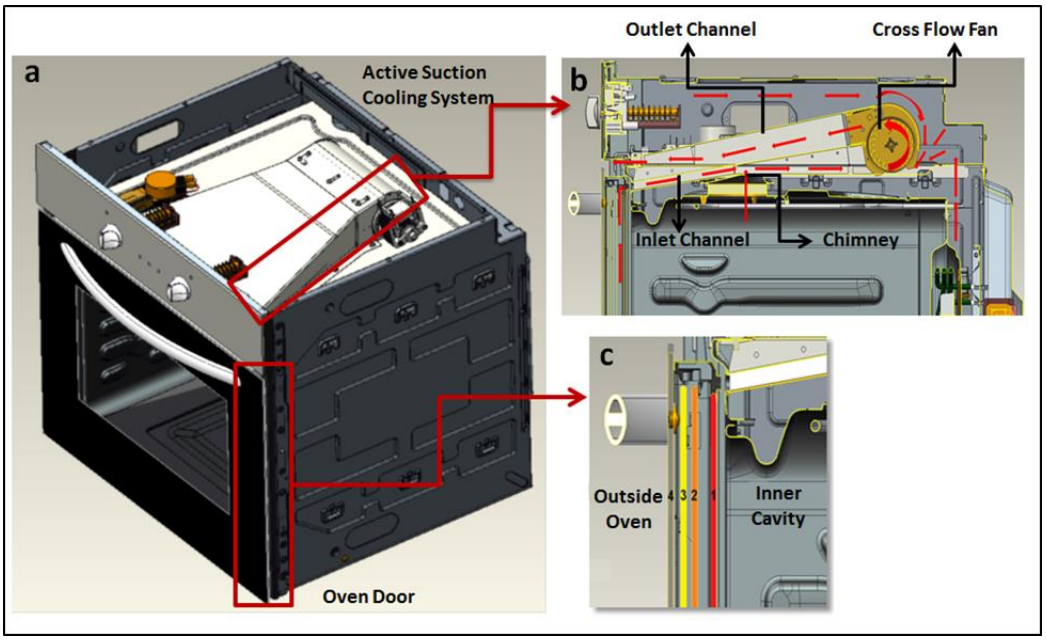

Figure 4.1 Pyrolytic oven views; (a) pyrolytic oven assembly, (b) active suction cooling system, (c) oven door

4.2 The Steady State Analysis of the Oven Door

The steps of the analysis of the oven door are as follows:

Preparing the cad model of the oven door,

Meshing of the oven door,

Boundary conditions of the oven door,

Solver of the oven door

4.2.1 Preparing CAD Model for Numerical Study

The first analysis of this study is concerned with the oven door which is shown in Figure 4.2. A door model which consist quadruple glass was prepared for this study. The model has four glass, air which gets between the panes of door and plastic profile which holds the glass together.

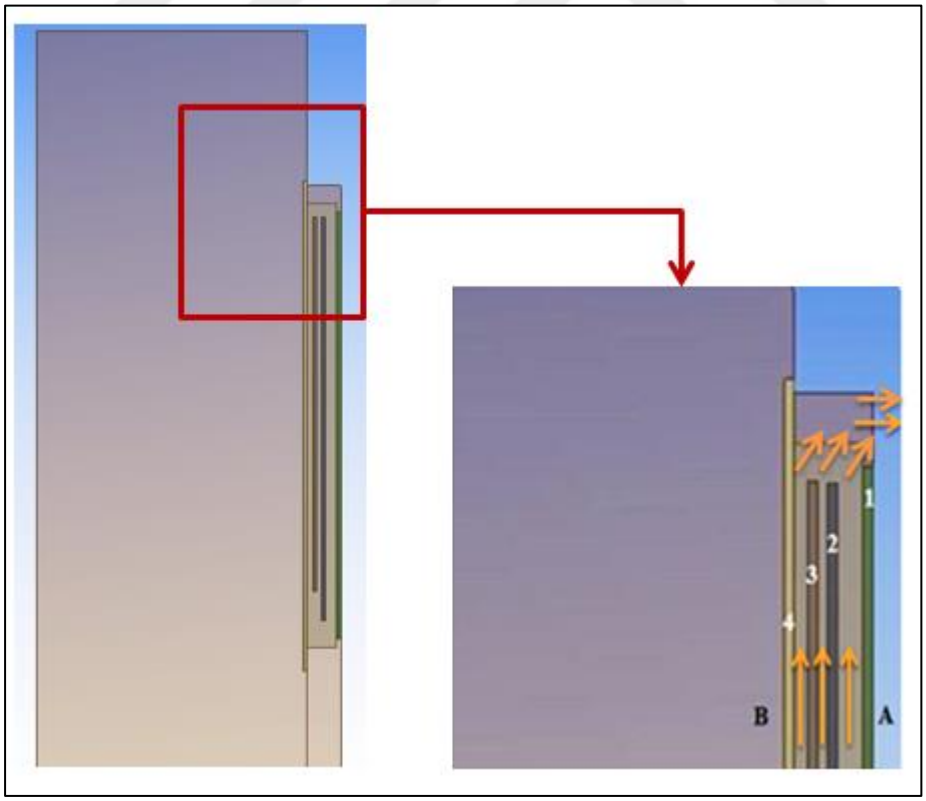

Figure 4.2 Oven door glass and air circulation of the oven door

ASC system gets air between the panes of door glass and from the chimney of the oven. The numerical model is shown in Figure 4.2. The “A” side shown in Figure 4.2 is the oven inner cavity direction and the “B” side is the outside of the oven. Glass number 1 (inner glass 8 pane) is the pane that contacts with the oven inner cavity and glass number 4 (outer glass pane) contacts with the ambient atmosphere of the oven.

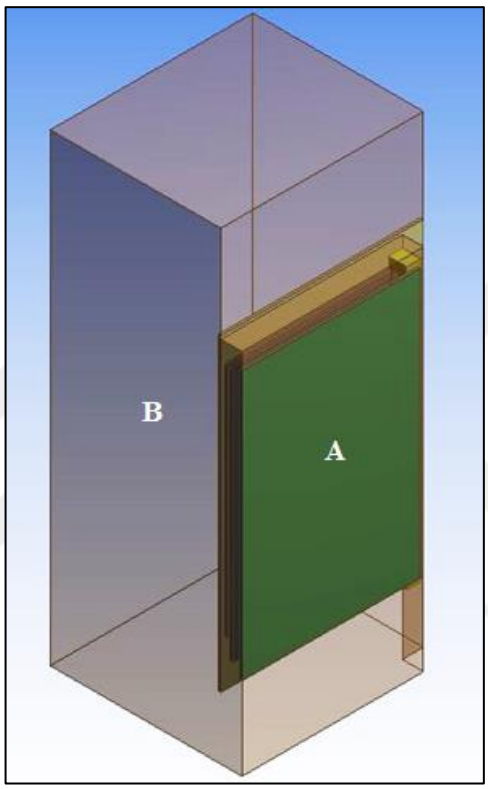

Figure 4.3 Numerical model of oven door

As seen from Figure 4.3, the oven door has been created as half model for simplification reasons since the air flow in the door has been considered as symmetrical. For modeling the ambient air and seeing the ambient air movements 250 mm thickness of air was created. For determining this value different thickness were studied and selected the optimal thickness of ambient air by Kilic (2014).

4.2.2 Meshing of the Oven Door

The meshing process is the most important step of CFDHT study. Because of this meshing process must be done properly to achieve the closest results.

Oven door is comprised of very small and very large entities. Air gaps between the glass panes, glass thicknesses are very small entities comparing to ambient air cavity. Because of these reasons meshing process need detailed attention to get best results.

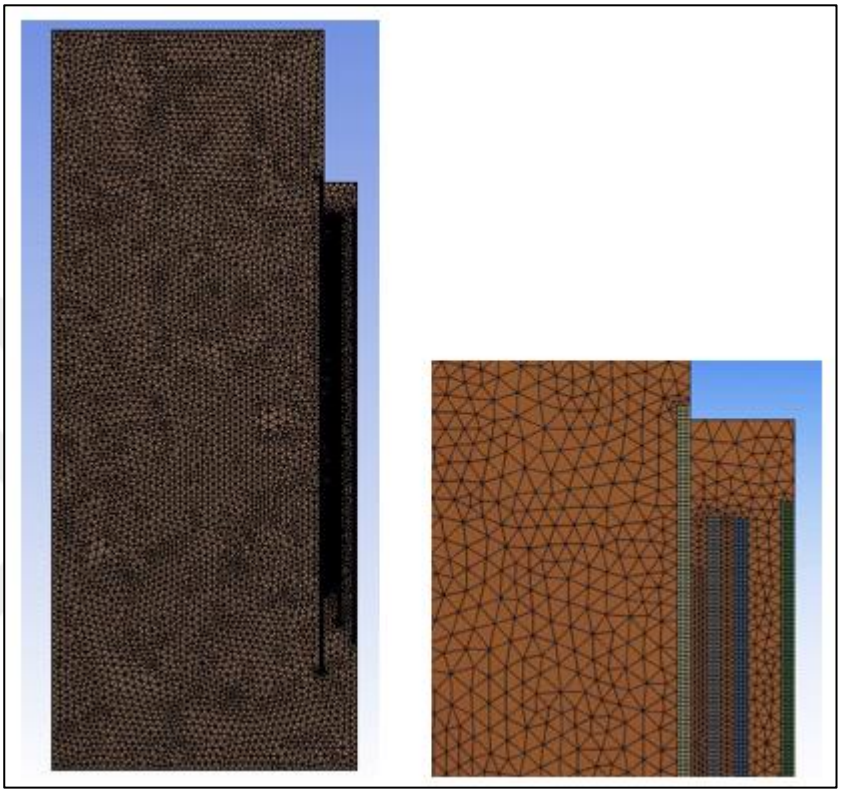

Figure 4.4 Mesh structure of the oven door

Glasses of the oven door and distances between glasses (air gaps) have small entities, so that the element sizes should be small for these regions. In these regions have been meshed with a body sizing option, the body of the ambient air volume of the rest of door has been meshed normally. Mesh structure of the oven door is shown in Figure 4.4.

Before preparing mesh settings, the names of oven door model's regions were defined for the ease of definitions of boundary condition. Mesh quality was checked and surfaces, bodies were named for the ease of definitions.

The generated mesh has 3331689 tetrahedral elements and 1744794 nodes.

4.2.3 Boundary Conditions of the Oven Door

The prepared numerical model was transferred to the CFD program for the preprocessing. Model of oven door has one fluid (air) domain, five solid (four glasses and one plastic profile) domains that were introduced to the program. Thermo-physical properties of the glass plate which are used in prototype shown in Table 4.1. These values were used to describe glass. Thermophysical properties of the plastic profile are shown in Table 4.2.

Table 4.1 Thermophysical properties of the glass plate

Properties	Value
Density (kg/m^3)	2500
Poisson coefficient	0.2
Specific heat (kJ/(kg K))	0.72
Emissivity	0.837
Conductivity (W/(m K)	1

Table 4.2 Thermophysical properties of the plastic profile

Properties	Value
Density (kg/m^3)	910
Poisson coefficient	0.2
Specific heat (kJ/(kg K)	1.25
Emissivity	0.91
Conductivity (W/(m K)	0.45

These domains which are named as air and glass domains for simplicity are connected to each other with a fluid to solid domain interface option. Also, air and plastic profile domains are connected to each other with a fluid to solid domain interface option, too. Finally, plastic profile and glass domains are connected to each other with a solid to solid domain interface option.

The outer surface of the air model that is opening to ambient atmosphere was defined as opening boundary condition. Symmetry planes of the all bodies have also set at the required faces. Remaining faces which are not openings or symmetry

planes have been selected as no slip walls. Opening temperature is entered 25 ^{0}C. Also, buoyancy boundary condition is activated.

Figure 4.5 shows boundary definitions of the model.

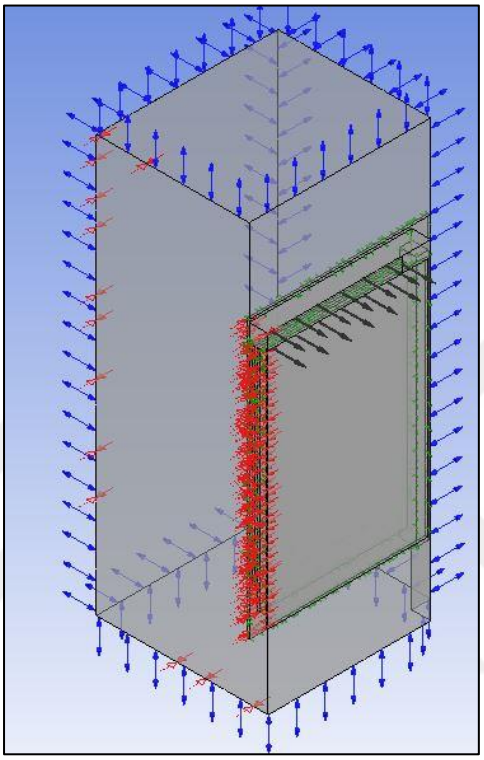

Figure 4.5 Definitions of the model

ASC system gets air by inflow channel. Air goes in the inflow channel by passing through the glass panes of the door. To simulate this flow velocity outlet boundary condition was defined to the surface that contacts with the inflow channel. Air gets in the door from ambient atmosphere and goes out to the inflow channel of active suction system. The velocity value 3 m/s was obtained as a result of the experiments.

Inner cavity of the oven was not modeled so temperature value which is obtained from the experiments defined to first glass inner surface that intersects with the oven inner cavity. Emissivity coefficient of the all surfaces and interfaces was obtained. The surfaces that contact to the oven upper panel and the remaining surfaces were defined as wall.

The analysis has been made with steady-state assumption. Also, thermal heat transfer mechanism was chosen.

4.2.4 Solver of the Oven Door

After the definitions of boundary conditions and initial conditions, solver control definitions were made. Three dimensional, steady-state analyses' iterations have continued until residuals reach 10*E-6 and domain H-energy imbalances come below % 0.01. The analysis has been completed in 654 iterations and residuals for the analysis have been shown in Figure 4.6, Figure 4.7 and Figure 4.8.

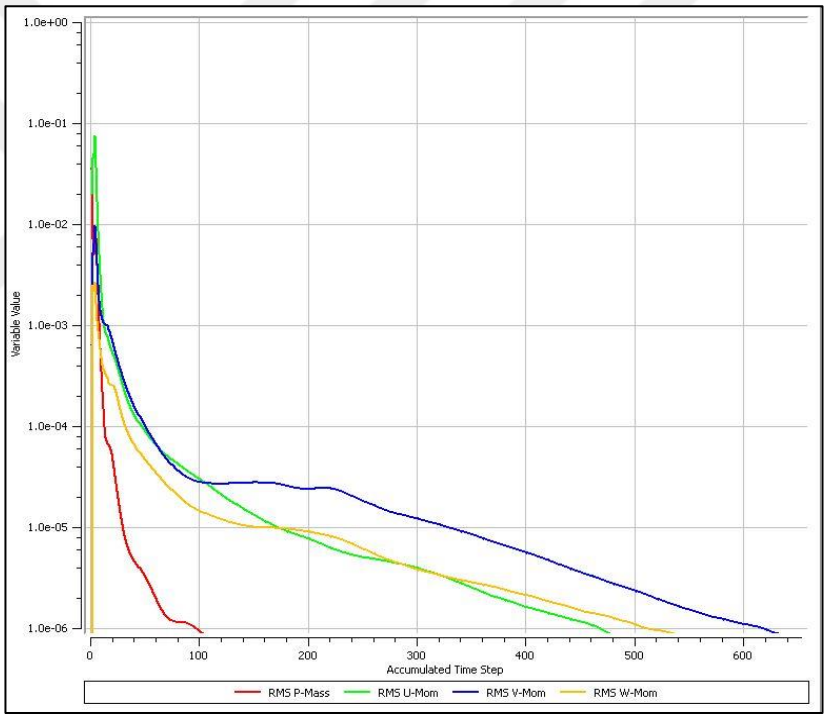

Figure 4.6 Momentum and mass residuals

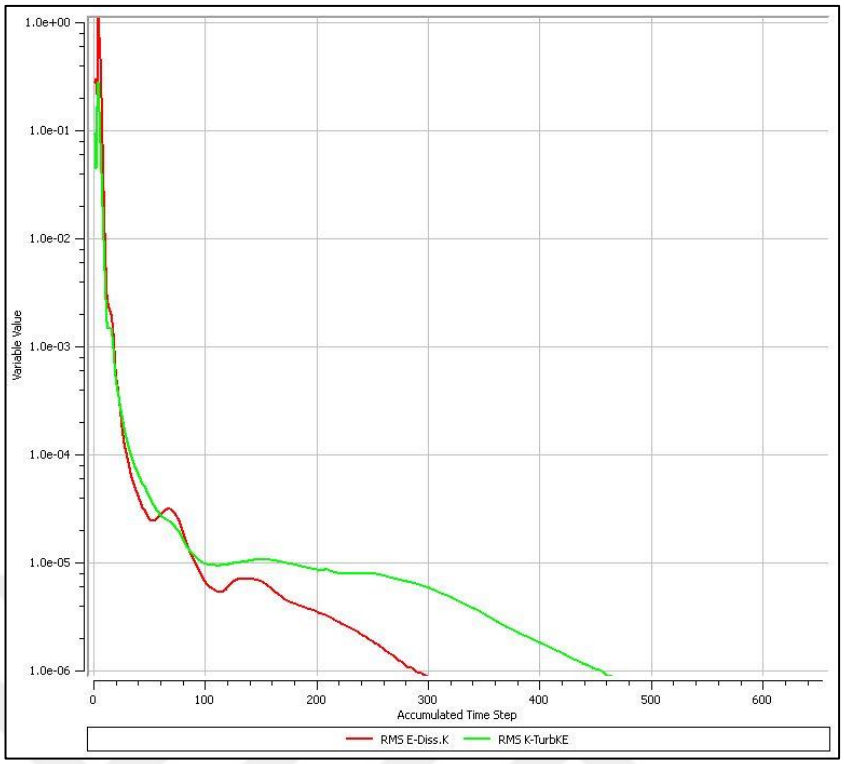

Figure 4.7 Turbulence residuals

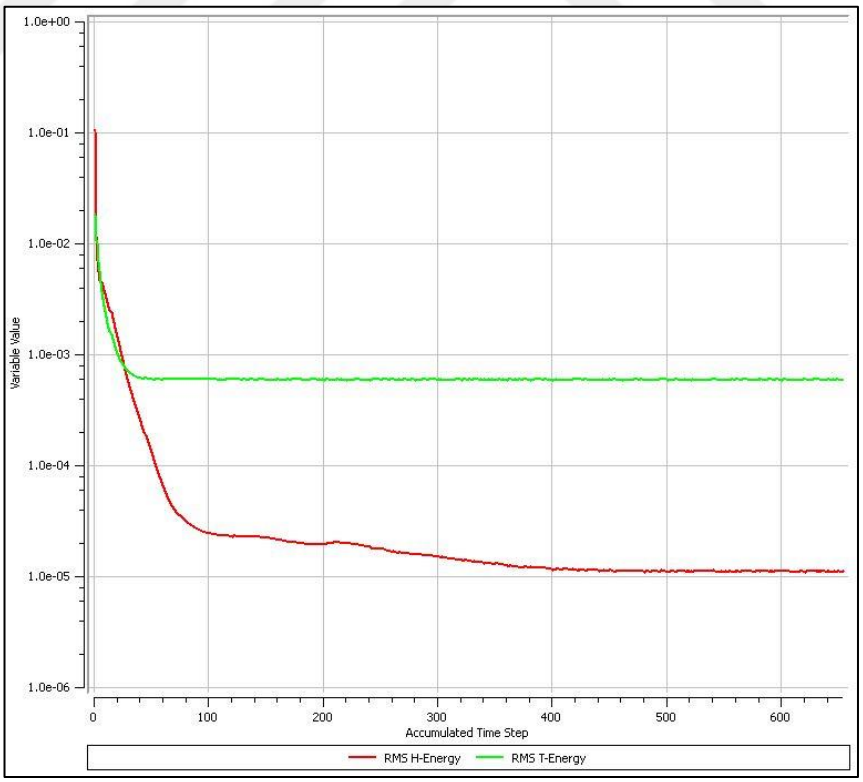

Figure 4.8 Heat transfer residuals

4.3 Steady State Thermal Analysis of the Ovens Door and ASC System

The steps of the analysis of the oven door and ASC system are as follows:

Preparing the cad model of the oven door and ASC system,

Meshing of the oven door and ASC system,

Boundary conditions of the oven door and ASC system,

Solver of the oven door and ASC system

4.3.1 Preparing the Cad Model of the Oven Door and ASC System

The second analysis of this study is concerned with the oven door and ASC system. The main purpose of the active suction system is to actively cooling the oven's door by drawing the air between the oven's glasses. Active suction of air is provided by the CFF which is in the ASC unit. Another purpose of the CFF of this unit is drawing the air from the oven cavity through the chimney of the cavity.

As it is mentioned, the main purpose of the ASC system is to actively cooling the oven's door by drawing the air between the oven's glasses. Suction of air is provided by the CFF which is in the ASC unit. The air volume of the unit has been prepared with a modeling program according to the CAD model of the oven with necessary simplification and has been shown in Figure 4.9a. For modeling the ASC system, inlet and outlet channels, chimney area and fan were modeled. The system has two bodies which are CFF and air cavity. Model of CFF is shown in Figure 4.9b and Figure 4.9c.

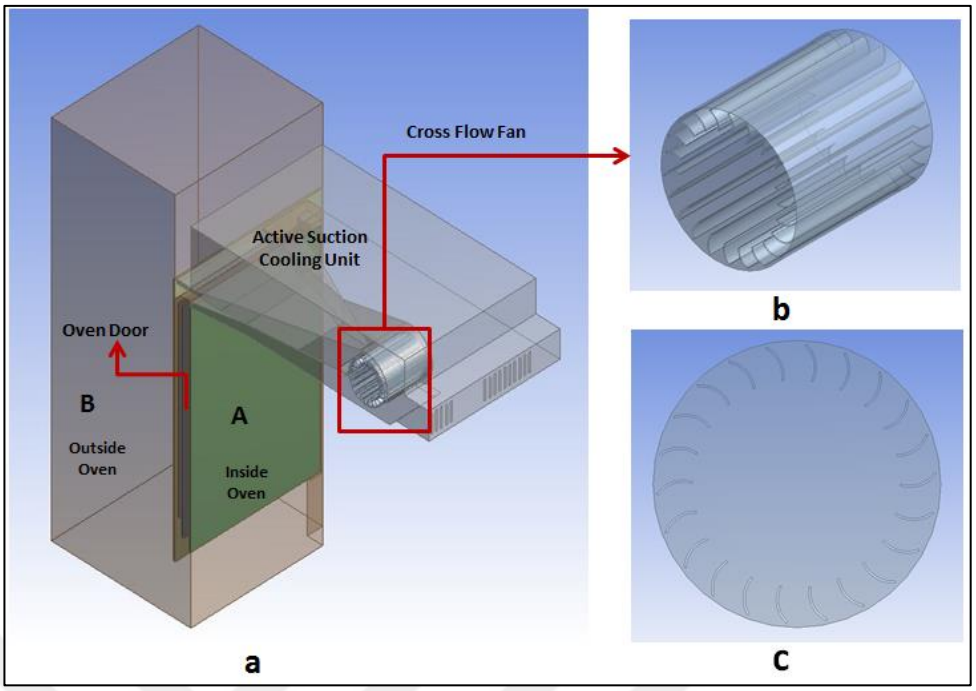

Figure 4.9 3D numerical model; (a) model of oven door and ASC system, (b) model of CFF air, (c) detail of CFF air

For modeling the ASC system, inflow and outflow channels, chimney area, back side of the ASC system and fan was modeled. Model of ASC system has two bodies which are CFF and air cavity. The model, which is investigated in this step, has ASC unit, CFF and oven doors' model. Oven door was modeled in chapter 4.2. Oven door and ASC system was investigated together in this chapter.

4.3.2 Meshing of the Oven Door and ASC System

The most important steps to reach the closest results to real life in a CFDHT analysis are generating a proper numerical grid model correctly. Mesh structure of the system are shown in Figure 4.10a. Glasses of the oven door and distances between glasses (air gaps) have small entities, so that the element sizes should be small for these regions. In these regions have been meshed with a body sizing option, the body of the ambient air volume of the rest of door has been meshed normally as shown in Figure 4.10b. Fins of the fan are very small comparing to air cavity. So that different domains meshed by different elements sizes. Mesh details of fan is shown in Figure 4.10c and Figure 4.10d.

For defining the optimum number of mesh element models that have 5273651, 10285361, and 30224854 number elements have been created. After getting results from these models, the model which has 5273651 number elements chosen for final

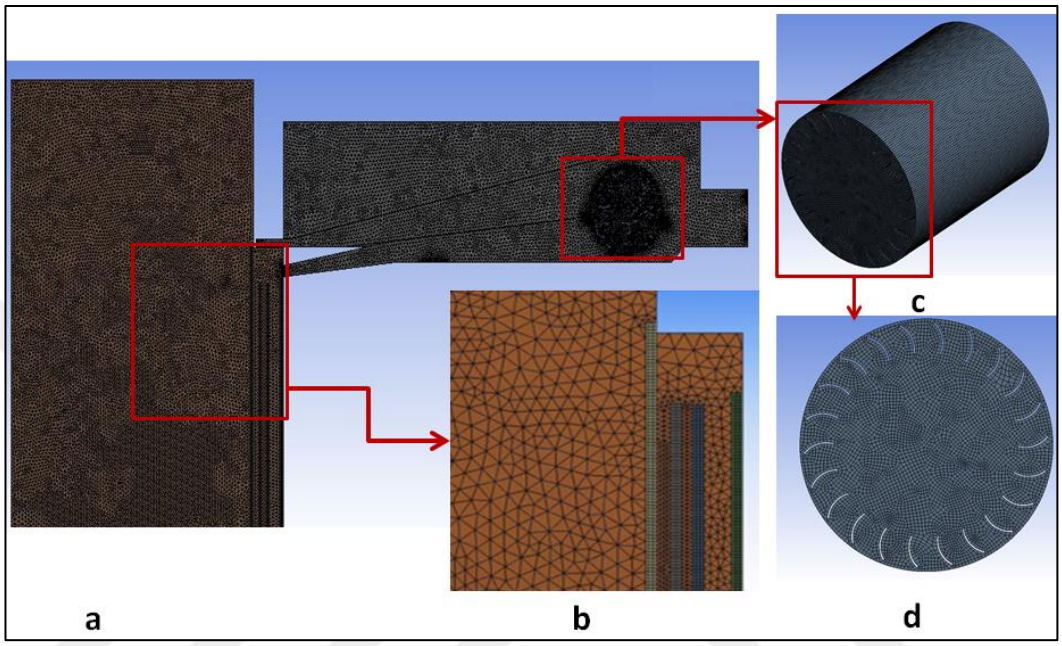

Figure 4.10 Mesh details of the numerical model; (a) mesh detail of oven door and active suction system, (b) mesh detail of oven door, (c) mesh detail of fan, (d) front view of fans' mesh detail

4.3.3 Boundary Conditions of the Oven Door and ASC System

After preparing the mesh, model is transferred to pre-processing module. The model has four glasses, doors' air, one doors' profile, air of ASC unit and one CFF air. There are seven stationer and one rotating domains. Air of oven door and CFF unit, glasses and profile are the stationary domains and fan is the rotating domain. Analysis type was steady state. Rotating speed of fan is 2400 rpm. This value was defined as boundary condition. Inlet of the ınflow channel, outlet of the outflow channel and chimney surface defined as opening. Since the model was half, symmetry faces was defined to the symmetry boundary condition. Since we had named the surfaces and bodies defining boundary conditions gets easier.

Air of oven doors and glass domains for simplicity are connected to each other with a fluid to solid domain interface option. Also, air and plastic profile domains are connected to each other with a fluid to solid domain interface option, too. Plastic profile and glass domains are connected to each other with a solid to solid domain interface option. Figure 4.11 shows boundary definitions of the model.

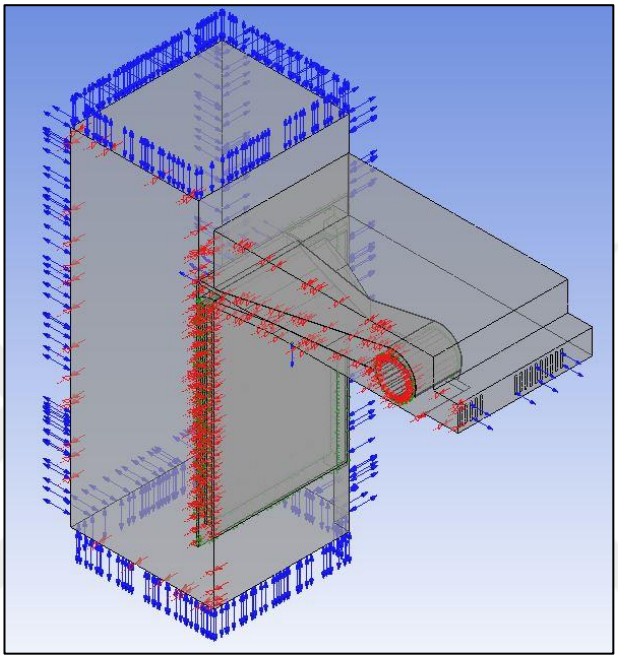

Figure 4.11 Definitions of the model

4.3.4 Solver of the Oven Door and ASC System

After determining the boundary conditions and setting up the initial conditions, solver control definitions have been made with the program's solver module. The analysis has been completed in 810 iterations and residuals for the analysis have been shown in Figure 4.12, 4.13 and 4.14.

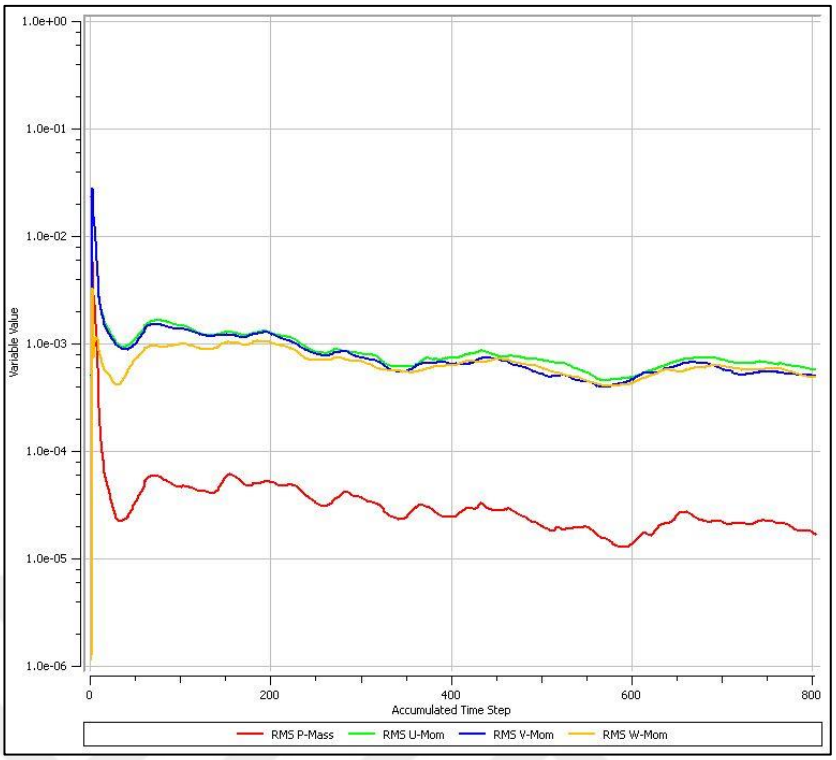

Figure 4.12 Momentum and mass residuals

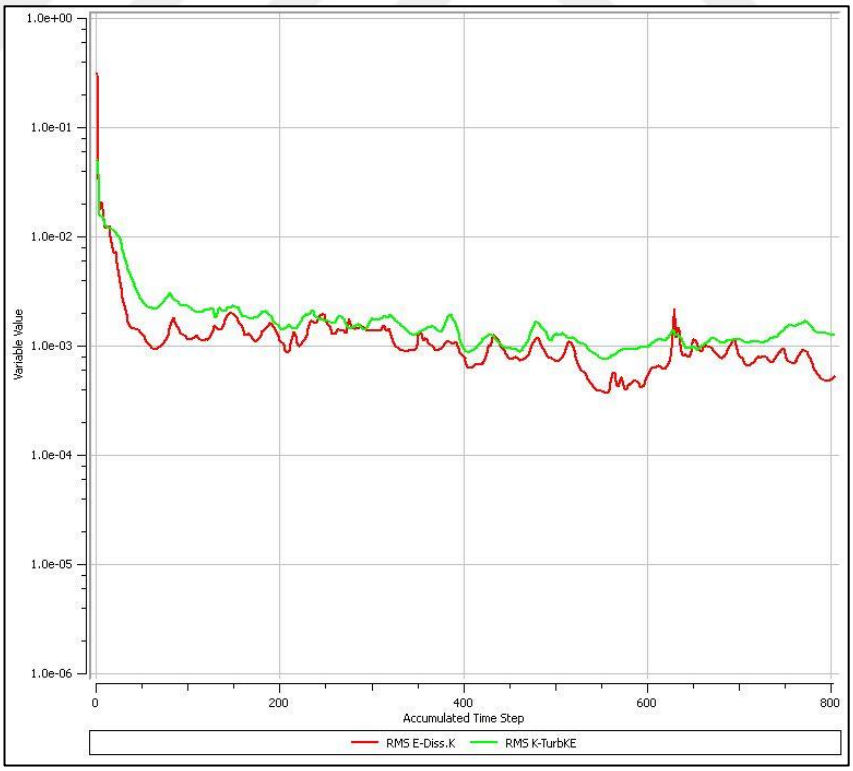

Figure 4.3 Turbulence residuals

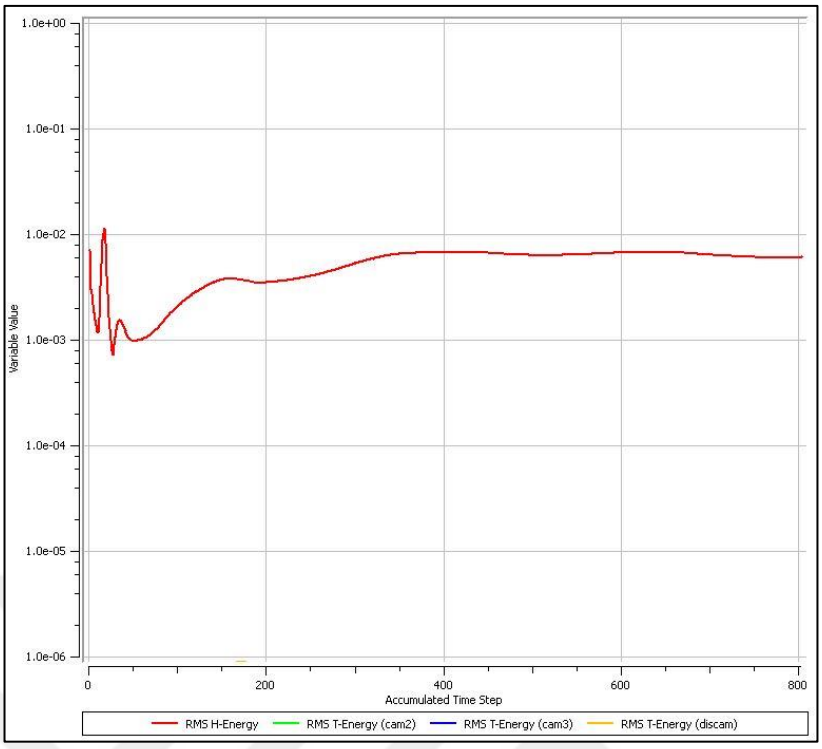

Figure 4.4 Heat transfer residuals

4.4 Validation of Numerical Study

To validate the velocity field, experiments were done and compared to the CFDHT analysis for obtaining more reliable results. In the experiment, eleven out of sixteen of the hot wire anemometers have been placed on the air flow inlet of the unit. The rest of the anemometers have been placed on the air flow outlet of the unit. When the system reached a steady state, air flow data have been recorded every 0.3 second over the duration of approximately five minutes. After completing the experiments, average flow data of the entire inlet and outlet of the unit have been obtained to validate the numerical study. The positions of the anemometers for the velocity measurements at ASC system are given in Figure 4.15.

Figure 4.15 Arrangement of anemometers in experimental study

Figure 4.16a is shown fluid flow of the ASC system and oven door. The fan drives the ambient air between oven glasses and blows air through the outlet channel. Then the air is driven out from upper oven door. The fan suctions ambient air from between oven glasses and blows air from upper oven door. Figure 4.16b shows velocity vectors of suction and discharge opening.

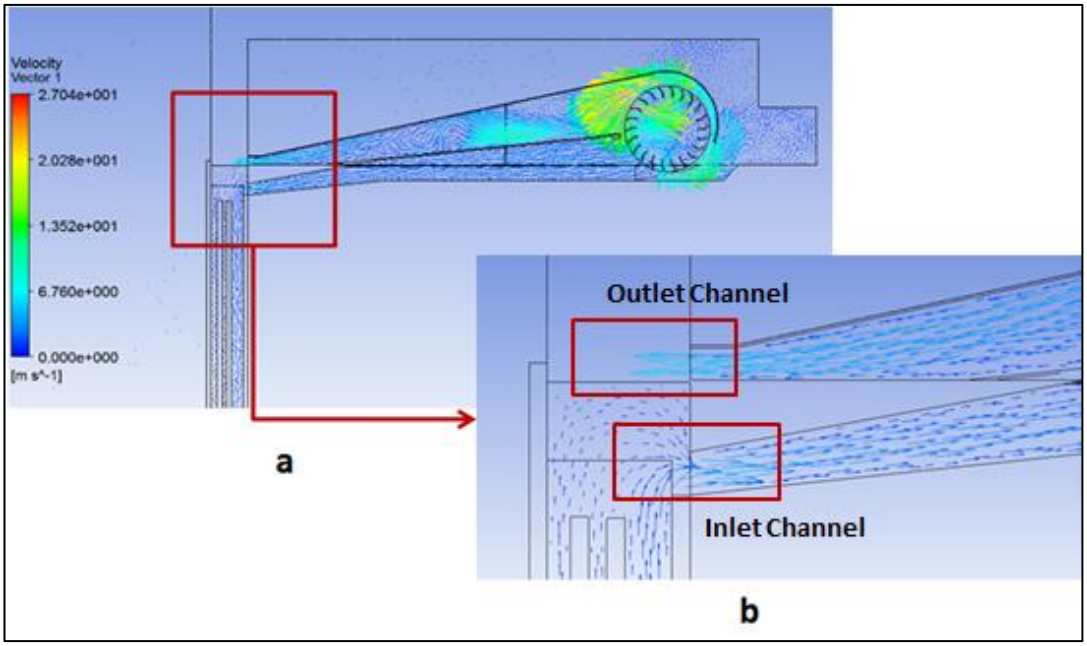

Figure 4.16 CFD results; (a) fluid flow of ASC system and oven door, (b) fluid flow of the inlet and outlet ASC system

Table 4.3 Comparison of the computational and the experimental studies for the inlet and outlet channel of ASC unit

Average velocity (m/s)	Experimental study	Numerical study	Absolute Difference
Inlet	3.07	2.98	0.09
Outlet	7.78	6.92	0.86

Average velocity of suction opening which in ASC system unit is 2.98 m/s. Also, average velocity of outlet of active suction system unit is 6.92 m/s. Differences of experimental and numerical studies are shown in Table 4.3. These results are similar to experimental results. Finally, CFD studies were validated with experimental studies.

Temperature experiment was done during the pyrolytic cycle which is continuing 1.5 hours. During the all experiments ambient temperature was 25˚C. Surface temperature of the outer glass door was measured via digital thermometer at three minutes before the completion of the cycle. In addition, the surface temperature distribution was obtained via the thermal camera. The temperature data obtained by the thermal camera and digital thermometer were used to validate numerical study.

Figure 4.17a is shown temperature distribution of the outer ovens' surface in the experimental study. The temperature measuring values (T1, T2,…, T12) were the maximum temperatures values of the area (Figure 4.17a). In the numerical study, temperature distribution of the outer oven doors' surface is in Figure 4.17b.

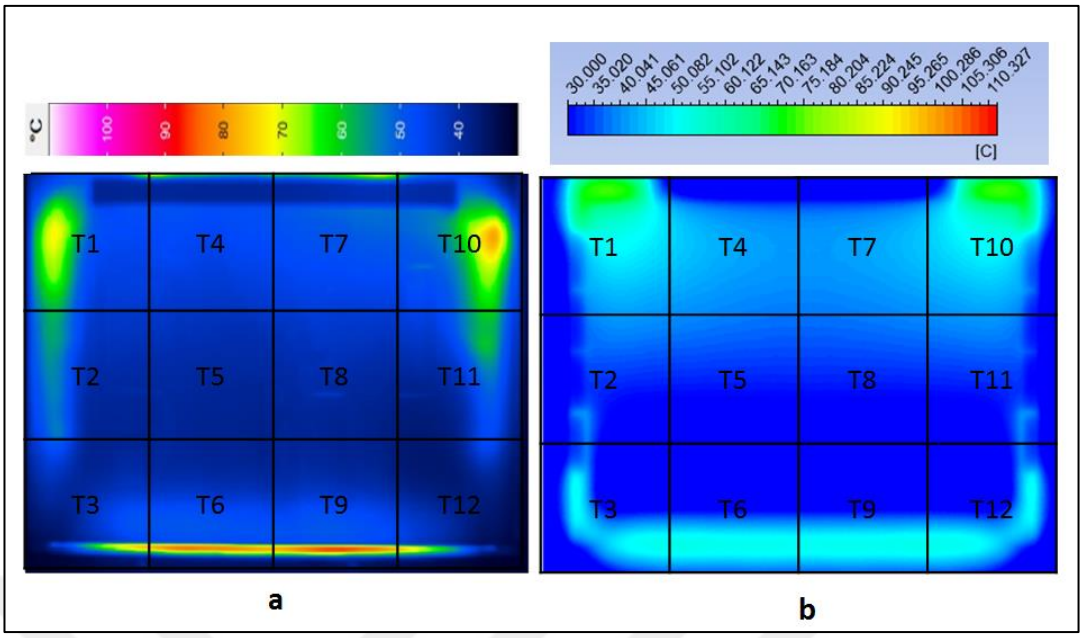

Figure 4.17 The temperature distribution of the outer surface of oven door; (a) experimental results, (b) computational results

Table 4.4 shows that the comparison of the experimental and numerical result for the maximum temperature of the temperature points. For the temperature points, the maximum relative error is 4.42%. It can be observed that the relative error values are in the range of 0-4.42 %.

Table 4.4 Comparison temperature results

Temperature of test data	Experimental Results (°K)	Numerical Results (°K)	Error (%)
T1	343	358	4,37
T2	330	334	1,21
T3	325	338	4,00
T4	317	321	1,26
T5	312	312	0,00
T6	320	331	3,44
T7	321	321	0,00
T8	311	312	0,32
T9	317	331	4,42
T10	352	358	1,70
T11	332	334	0,60
T12	324	338	4,32

A scatter plot of the comparison between the numerical result and experimental results for temperature points, are shown in Figure 4.18. In the study of Mistry, Ganapathisubbu, Dey & Castillo (2006), it is mentioned that these differences are within acceptable limits, so that the numerical results have been concluded to be reliable

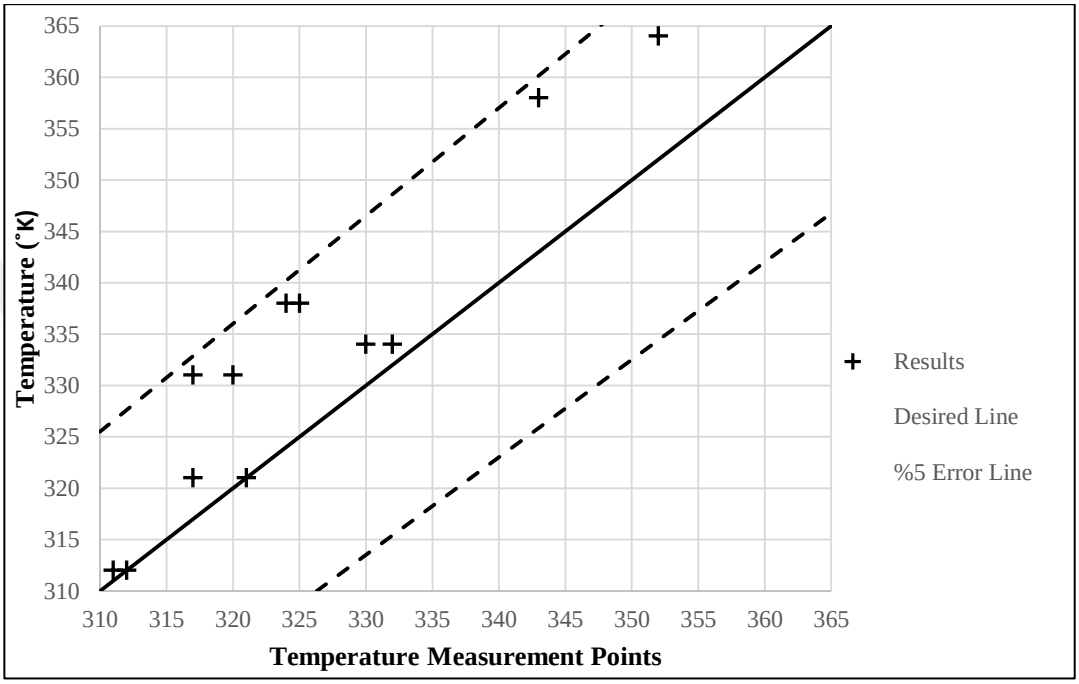

Figure 4.18 Temperature comparisons between experimental and computational results

Finally, it is shown that the predicted results are close to experimental data by numerical approach. The Numerical results reveal that the oven door and ASC system can be modeled using the numerical study rather than the experimental study in order to estimate its parametric study.

4.5 Parametric Study

4.5.1 Effect of Rotational Speed of CCF

At the oven door heat transferred is by conduction, convection and radiation. In the oven cavity the air is heated by heaters and it circulates in the oven. At pyrolytic type ovens radiation is the dominant heat transfer mechanism because of the high

temperatures. Radiation that is emitted by the heaters causes that the door cavity heat up and active suction system causes to cool down the door cavity by convection. To see the effect of CFFs' rotational speed, Reynolds number was calculated according to Equation 4.1 and 4.2. The Reynolds number according such as (n) rotational speed of fan (rpm), (D) impeller external diameter (mm), (c_p) blade chord (mm) and (v) kinematic viscosity (m^2/s) were calculated.

$$Re = \frac{U_L.C_p}{v} \tag{4.1}$$

$$U_L = \frac{2.\pi.n}{60}.\frac{D}{2} \tag{4.2}$$

Figure 4.19 shows the effect of Reynolds number (Re) on the temperature of oven doors' surface. The first vertical axis shows the outer average temperature of fourth glass in Kelvin, the second vertical axis shows the average velocity of inlet and outlet channel in m/s. Horizontal axis shows Reynolds number.

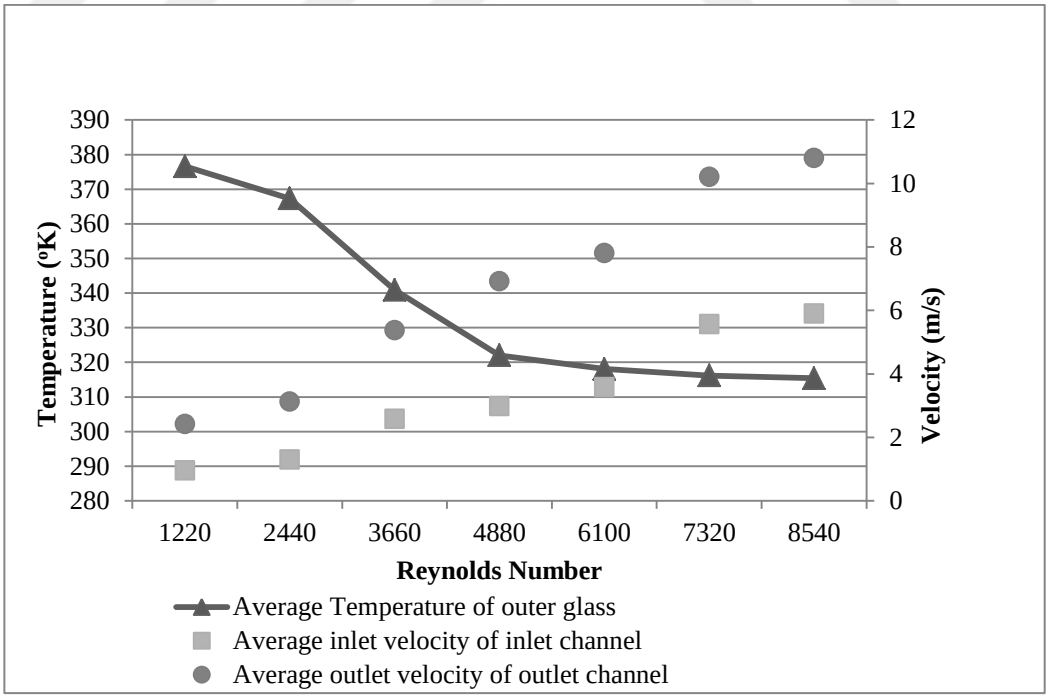

Figure 4.19 The effects of speed of the cross flow fan on the outer surface of oven door

The increase of the Reynolds number depends on the fan rotational speed. As shown in Figure 4.19, minimum temperature was acquired when Re was 8540. After a specified value, which is 4880, there are no noticeable effects on temperature of oven doors' outer surface.

CHAPTER FIVE
CONCLUSIONS

The aim of this study is to investigate the heat transfer and fluid (air) flow characteristics of domestic ovens which has active suction cooling system by implementing numerical methods. A prototype pyrolytic domestic oven has been used in these studies. In literature researches, both of numerical and experimental studies for investigating the heat transfer and air flow inside oven and oven door. Door of a domestic oven and its upper fan that provides active air suction from door unit were modelled using the computational fluid dynamic and heat transfer (CFDHT) method. The numerical results were validated by comparing with the results obtained from experimental study. Studies were temperature and velocity distribution inside the oven cavity. Some studies were on industrial ovens. Only a few ones are about oven door and heat transfer mechanism in the door.

In this thesis, two different three dimensional numerical models of both the oven door and all of the ASC system were prepared and CFDHT analyses were made. Oven door and ASC system were modelled three dimensional first times in this study and parametric studies were done. Firstly, ASC system was modeled and fluid flow was investigated. Then, oven door and ASC system were modeled together and temperature distribution of outers' oven door was investigated. As a contribution to the literature, Reynolds number was investigated by parametrically.

It is possible to reduce prototype costs and times by implementing this method. The effects such as changing the model fan case or selecting a different insulation type can be done numerically to examine the possible results by implementing similar analyses.

REFERENCES

Abraham, J.P., & Sparrow, E., M. (2004). A simple model and validating experiments for predicting the heat transfer to a load situated in an electrically heated oven. *Journal of Food Engineering 62*, 409–415.

Alvarez, G., Flores, J. J., Aguilar, J. O., Go´mez-Daza, O., Esrada, C. A., & Nair, M. T. S, et al. (2005*).* Spectrally selective laminated glazing consisting of solar control and heat mirror coated glass: preparation, characterization and modeling of heat transfer. *Solar Energy 78*, 113–124.

Bergman, T. L., Lavine, A. S., Incropera, F. P., & DeWitt, D. P. (2012*).* *Fundamentals of heat and mass transfer* (7th ed.). USA: John Wiley & Sons.

Blazek, J. (2001). *Computational fluid dynamics: Principles and applications*. Netherlands: Elsevier Science Ltd.

Chhanwal, N., Anishaparvin, A., Indrani, D., Raghavaro, K.S.M.S., & Anandharamakrishnan, C. (2010). Computational fluid dynamics (CFD) modelling of an electrical heating oven for bread-baking process. *Journal of Food Engineering. 100*, 452–460.

Chhanwal, N., Indrani, D., Raghavaro, K.S.M.S., & Anandharamakrishnan, C. (2011). Computational fluid dynamics modeling of bread baking process. *Food Research International 44*, 978–983.

Çengel, Y. A., & Boles, M. A. (2006). *Thermodynamics an engineering approach* (5th ed.). New York: McGraw-Hill.

Fahey, M., Wakes, S. J., & Shaw, C. T. (2008). Use of computational fluid dynamics in domestic oven design. *The International Journal of Multiphysics 1*, 37-57.

Fan, Y., Hyde, T., Hewitt, N., Eames, P.C., & Norton, B. (2009). Comparison of vacuum glazing thermal performance predicted using two-and three-dimensional models and their experimental validation. *Solar Energy Materials & Solar Cells 93,* 1492–1498.

Ganapathisubbu, S., Dey, S., Bishnoi, P., & Castillo, J.L. (2006). Modeling of transient natural convection heat transfer in electric ovens. *Applied Thermal Engineering 26,* 2448–2456.

Kilic, I. (2014). *Optimizing the design parameters of oven door.* M.Sc. Thesis, Dokuz Eylül Üniversitesi, İzmir.

Lazzarotto, L., Lazzarotto, A., & Martegani, A.D. (2001). On Cross-Flow Fan Similarity: Effects of Casing Shape. *Journal of Fluids Engineering 123,* 523–531.

Mistry, H., Ganapathisubbu, S., Dey, S., Bishnoi, P., & Castillo, J.L. (2006). Modeling of transient natural convection heat transfer in electric ovens. *Applied Thermal Engineering 26,* 2448–2456.

Mistry, H., Ganapathisubbu, S., Dey, S., Bishnoi, P., & Castillo, J.L. (2011). A methodology to model flow-thermals inside a domestic gas oven. *Applied Thermal Engineering 31,* 103-111.

Rek, Z., Rudolf, M., & Zun, I. (2012*).* Application of CFD Simulation in the Development of a New Generation Heating Oven*. Strojniški vestnik - Journal of Mechanical Engineering 58,* 134-144.

Shaughnessy, B. M., & Newborough, M. (2000). Energy performance of a low-emissivity electrically heated oven. *Applied Thermal Engineering 20,* 813-830.

Smolka, J., Nowak, A. J., & Rybarz, D. (2009). Improved 3-D temperature uniformity in a laboratory drying oven based on experimentally validated CFD computations, *Journal of Food Engineering 97*, 373–383.

Therdthai, N., Zhou, W., & Adamzack, T. (2004). Three-dimensional CFD modeling and simulation of the temperature profiles and airflow patterns during a continuous industrial baking process. *Journal of Food Engineering 65*, 599-608.

Unsalan, D. (2014). *Numerical and experimental investigations of heat transfer and fluid flow analyses of domestic ovens.* M.Sc. Thesis, Dokuz Eylül Üniversitesi, İzmir.

Verboven, P., Scheerlinck, N., Baerdemaeker, J., & Nicolai, B. M. (2000a). Computational fluid dynamics modeling and validation of the temperature distribution in a forced convection oven. *Journal of Food Engineering 43*, 61-73.

Verboven, P., Scheerlinck, N., Baerdemaeker, J. D., & Nicolai, B. M. (2000b). Computational fluid dynamics modeling and validation of the isothermal airflow in a forced convection oven. *Journal of Food Engineering 43*, 41-53.